Proc. Natl. Acad. Sci. USA
Vol. 86, pp. 4425–4429, June 1989
Biochemistry

Mismatch repair involving localized DNA synthesis in extracts of *Xenopus* eggs

(heteroduplex DNA/DNA-repair intermediates/mutagenesis/recombination)

PETER BROOKS, CHRISTIANE DOHET, GENEVIÈVE ALMOUZNI, MARCEL MÉCHALI, AND MIROSLAV RADMAN*

Institut Jacques Monod, Centre National de la Recherche Scientifique, Tour 43, 2 place Jussieu, 75251 Paris Cedex 05, France

Communicated by Maxine F. Singer, March 22, 1989 (received for review October 14, 1988)

ABSTRACT **Repair of heteroduplex DNA containing G·T or A·C mismatches or containing two tandem unpaired bases occurred *in vitro* with *Xenopus* egg extracts as detected by a physical assay. The repair was accompanied by a mismatch-stimulated and mismatch-localized DNA synthesis. Repaired molecules, separated from unrepaired molecules, showed a 20- to 100-fold increase in DNA synthesis in the region of the mismatch compared to regions distant from the mismatch. The remaining unrepaired heteroduplex DNA included molecules that also displayed mismatch-stimulated DNA synthesis in the mismatch-proximal regions. These may represent intermediates in the repair process. The patterns of DNA synthesis suggest that repair begins at some distance from the mismatch and that as much as 1 kilobase or more can be involved in the mismatch-stimulated synthesis.**

Mispaired or unpaired bases in DNA can arise *in vivo* by at least three different mechanisms: (*i*) DNA replication errors, (*ii*) deamination of 5-methylcytosine to thymine creating a G·T mismatch, and (*iii*) events that result in the pairing of homologous but nonidentical sequences, such as in genetic recombination or in the formation of cruciform structures with imperfect palindromes. Two global mismatch-repair mechanisms have been well characterized in *Escherichia coli* and in *Streptococcus pneumoniae*: very short patch mismatch repair (VSPMR), involved in the repair of 5-methylcytosine deamination, and long patch mismatch repair (LPMR) (1–4).

The involvement of LPMR in the maintenance of genetic information during DNA replication and recombination and the role of VSPMR in the conservation and diversification of genetic information have been described (5, 6). The size of eukaryotic genomes and the density of 5-methylcytosine in most eukaryotic genomes suggest a requirement for both LPMR and VSPMR. Mismatch repair was first postulated by Holliday (7) to account for some aspects of genetic recombination in eukaryotes, such as gene conversion or nonreciprocal genetic recombination. Marker-specific effects in meiotic recombination of yeast and fungi (8, 9) offered evidence for mismatch repair in eukaryotes and, indeed, mismatch repair was observed in cell-free extracts of yeast (10). In contrast, there are no genetic studies that predict mismatch repair in the metazoa. Several reports of heteroduplex DNA transfections (11–13) suggest some mismatch-repair process in mammalian cells, but without mismatch-repair mutants, alternative processes such as strand loss, asymmetric replication, mismatch-independent nick-translation, and genetic recombination were not excluded (2, 3).

To study vertebrate mismatch repair *in vitro*, we chose extracts of *Xenopus laevis* eggs because they might be expected to have high levels of DNA-repair activities. *Xenopus* oocytes and eggs contain high levels of biosynthetic machinery, including reserves of enzymes and substrates sufficient to carry out the first 12 postfertilization cycles of DNA replication (14, 15). Moreover, the faithful conservation of the genome during early development is crucial. Here we report that heteroduplex DNA undergoes mismatch repair in *Xenopus* egg extracts.

MATERIALS AND METHODS

Egg Collection and Extraction. Eggs were collected and extracts were prepared by differential high-speed centrifugation as described (16) and stored at −80°C. The extracts contain endogenous cytoplasmic components diluted about 2-fold, including (as final concentrations) 50–70 μM dNTP (17) and about 3 mM ATP, and extraction buffer components: approximately 10 mM potassium Hepes (pH 7.5), 35 mM potassium acetate, 0.5 mM dithiothreitol, and 2.5% sucrose. Protein concentrations were 40–80 mg/ml. Before use, extracts were tested to assure their ability to replicate single-stranded DNA (ssDNA) and for the absence of excessive nuclease activities.

DNA Preparation and Heteroduplex Construction. Growth of *E. coli* JM110 (*dam dcm*), infection with M13 phage, and preparation of replicative form I (covalently closed circular double-stranded) DNA and ssDNA were as described (18). M13 mp2 form I was cleaved with *Ban* II or *Bam*HI and then mixed with a 10-fold molar excess of M13 mp1 ssDNA. Annealing and incubation with *E. coli* DNA ligase (New England Biolabs) were performed essentially as described (19). Covalently closed circular DNA was purified by CsCl/ethidium bromide centrifugation. Homoduplex DNA was prepared identically except with *Ban* II-cleaved mp2 form I plus mp2 ssDNA. Additional substrates (Fig. 1*a*) were prepared with *Ban* II- or *Bam*HI-cleaved mp1 form I and mp2 ssDNA, or with *Ban* II-cleaved mp2 form I and mp2B ssDNA, or with *Sal* I-cleaved mp18 form I and mp18N ssDNA. Both mp1/mp2 G·T and mp2/mp1 A·C heteroduplexes were resistant to *Eco*RI cleavage, the mp2B/mp2 T·G heteroduplex was resistant to *Bgl* II and *Acc* I, and the mp18N/mp18 2-base-addition heteroduplex was resistant to *Nru* I and *Sal* I. Radiolabeled substrates were prepared as described above except that form I mp2 DNA was linearized with *Bam*HI, annealed with either mp1 ssDNA or mp2 ssDNA, incubated with DNA polymerase I plus [α-^{32}P]dCTP and [α-^{32}P]dTTP (Amersham; 15,000 cpm/pmol in reaction) for 30 min at 12°C, and then treated with *E. coli* ligase. Distributive polymerization conditions resulted in synthesis of about 300 nucleotides per molecule. Unincorporated radiolabel was removed by centrifugational Sephadex G-50 sieving. The solution was adjusted to pH 12.3 with 175 mM NaOH, incubated at room temperature for 5 min, neutralized,

The publication costs of this article were defrayed in part by page charge payment. This article must therefore be hereby marked "*advertisement*" in accordance with 18 U.S.C. §1734 solely to indicate this fact.

Abbreviations: VSPMR, very short patch mismatch repair; LPMR, long patch mismatch repair; ssDNA, single-stranded DNA.

*To whom reprint requests should be addressed.

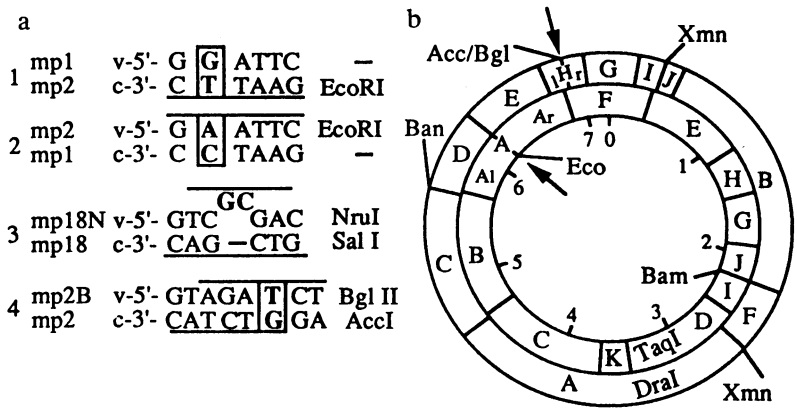

FIG. 1. Heteroduplex DNA substrates. (*a*) Mismatches studied and their positions in restriction enzyme sequences. M13 mp18N was made by digestion of mp18 with *Acc* I, end-filling, and ligation. M13 mp2B was made by replacing the 2.6-kilobase (kb) *Bsm* I–*Ban* II fragment of mp2 with that of mp18. v, Viral strand; c, complementary strand. (*b*) Restriction map of m13 mp2 (or mp2B). The positions for *Eco*RI, *Acc* I (mp2) or *Bgl* II (mp2B), *Xmn* I, *Ban* II, and *Bam*HI are indicated. The inner ring shows the fragments used for analyzing DNA synthesis in the mp1/mp2 substrates; the unlabeled cleavage positions are for *Taq* I. The outer ring shows the fragments for mp2B/mp2 analysis; the unlabeled positions are for *Dra* I. Fragment A for the *Taq* I digestion includes A_l and A_r, and fragment H for the *Dra* I digestion includes H_l and H_r. Arrows indicate mismatch positions.

adjusted to 0.8 M NaCl, and filtered through nitrocellulose (BA85; Schleicher & Schuell) by centrifugation at 1000 × *g* for 3 min to purify the covalently closed circular DNA.

Assay for Conversion of Mismatches to Normal Base Pairs. Incubation mixtures contained 1–200 μM homoduplex or heteroduplex DNA, [^{32}P]dNTP for some experiments, and 75–80 μl of egg extract per 100 μl, with no other additions. Buffers and salts were from the extract. Reactions were at 22°C for the times stated and were stopped by adjustment to 30 mM EDTA, 0.2% SDS, and 0.4 mg of proteinase K per ml; after 60 min at 37°C, the DNA was extracted with phenol/chloroform, 1:1 (vol/vol), and precipitated with ethanol. Then the DNA was linearized with *Bam*HI and probed with the restriction enzymes diagnostic for mismatch repair (Fig. 1*a*). Electrophoresis was in 1% agarose with 40 mM Tris acetate (pH 8.2), 1 mM EDTA, and 0.5 μg of ethidium bromide per ml. Gels included internal sets of standards of the 7.2-kb linear DNA and the repair-diagnostic fragments to estimate the extent of conversion to restriction enzyme sensitivity by ethidium bromide staining intensity (20).

Distribution of DNA Synthesis. The reaction mixtures were as above except with added [α-^{32}P]dATP and/or [α-^{32}P]dCTP. After postreaction purification as described above and addition of 0.8 μg of unlabeled mp2 DNA, the DNA was digested with the repair-diagnostic enzyme(s) and additional restriction enzymes to generate multiple fragments (Fig. 1*b*). Incorporation of radioactivity was determined by Cerenkov counting of excised gel segments. Autoradiography of dried gels showed the expected patterns of discrete bands. The specific incorporation in a fragment was calculated from its radioactivity and base composition. Relative specific incorporation is the ratio of specific incorporation of a given fragment to the specific incorporation of a designated fragment. Specific incorporation was also determined for the linear 7.2-kb DNA and the repair-diagnostic fragments and then normalized to the amount of DNA.

RESULTS

***Xenopus* Egg Extracts Restore Normal Base-Pairing in Heteroduplex DNA.** Based on the observation that a restriction site containing a single base-pair mismatch inhibits cleavage by the restriction enzyme (21), a physical assay for the conversion of heteroduplex DNA to homoduplex was developed (19). Mismatch-repair activity in *Xenopus* egg extracts was tested by this assay with the substrates shown in Fig. 1. For example, the M13 mp1/mp2 heteroduplex with a mismatch in the *Eco*RI site (Fig. 1*a*, substrate 1) was incubated with the extract, and the DNA was purified and linearized with *Bam*HI and then probed with *Eco*RI as the repair-diagnostic enzyme. In the absence of repair, only the linear 7.2-kb molecule is apparent. In contrast, when heteroduplex molecules are repaired (G·T to A·T) to give the normal *Eco*RI site, then the two *Bam*HI–*Eco*RI fragments (4.0 kb and 3.2 kb) are produced. Thus the appearance of these gel bands is diagnostic of mismatch repair.

When mp1/mp2 heteroduplex [^{32}P]DNA was incubated with the egg extract, repair to the *Eco*RI site was evident by the appearance of the diagnostic 3.2-kb band (Fig. 2, lanes 3c, 4c, 5c, and 6c). (The 4.0-kb diagnostic fragment does not appear on the autoradiogram because prelabeling by DNA polymerase was initiated at a nick at the *Bam*HI site with synthesis into the 3.2-kb fragment.) In this and other experiments using unlabeled DNA, repair increased through 30–60 min but no further increase was observed for up to 9 hr of incubation (Fig. 2 and data not shown). The reaction mixture contained a 200-fold excess of unlabeled mp2 DNA to compete for any nonspecific nucleases and to ensure complete recovery of DNA and complete digestion by the restriction enzymes as visualized by ethidium bromide staining. In the absence of excess mp2 DNA the same apparent rate and extent of activity were observed, implying that the activity acting on mismatches is highly specific for the heteroduplex DNA.

There were no differences between homo- and heteroduplex with respect to nicking, linearization, generation of higher molecular weight forms, substrate loss, or supercoiling (Fig. 2, lanes 3a, 4a, 5a, 6a, and 9a, and data not shown); in addition, no site-specific linearization of heteroduplex DNA was seen (Fig. 2, lanes 3b, 4b, 5b, and 6b).

Mismatches or Unpaired Bases Cause Localized DNA Synthesis. The activity that converted heteroduplex DNA to homoduplex DNA could have been due to a mismatch-stimulated process or to random strand-replacement synthesis that occasionally in some molecules passed through the mismatch site. For a mismatch-specific process, localized DNA synthesis might be expected. To test this prediction, unlabeled homoduplex DNA or heteroduplex DNA, with the mismatch at the *Eco*RI site, and [^{32}P]dNTP were incubated with the extract to determine the intramolecular distribution of DNA synthesis. The DNA was purified and then digested with *Bam*HI, *Eco*RI, and *Taq* I to generate fragments of an average size of about 400 base pairs (bp) (see Fig. 1*b*). This set of fragments includes the 1150-bp *Taq* I fragment A, containing the mismatch-bearing *Eco*RI site, and fragments A_l and A_r, generated by cleavage of the normally base-paired *Eco*RI site.

The net relative incorporation in fragments A, A_l, and A_r was higher than the incorporation in the remainder of the molecule (Fig. 3*a*). The relative specific incorporation value for the net synthesis in fragments A, A_l, and A_r was about 4; fragments A_l and A_r accounted for about 25% of this net synthesis but contained only about 1.3% of the net DNA in fragments A, A_l, and A_r, thus giving relative specific incor-

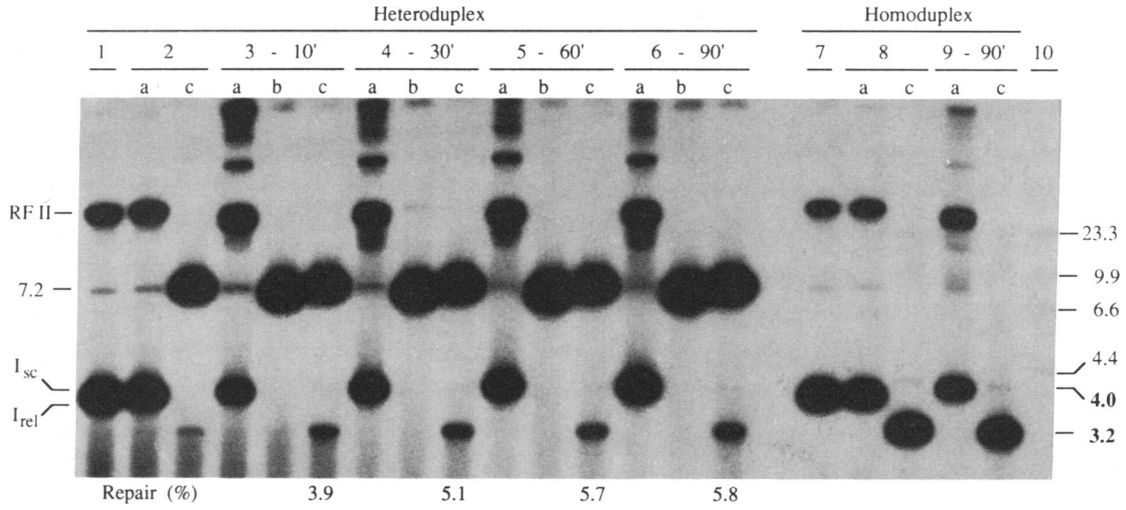

FIG. 2. *Xenopus* egg extracts convert heteroduplex DNA to homoduplex DNA. Reactions were with 1 μM ^{32}P-prelabeled DNA (prepared as described in *Materials and Methods*; homoduplex mp2/mp2 or heteroduplex mp1/mp2) and 200 μM unlabeled mp2 form I DNA; aliquots were removed at the times shown (10, 30, 60, or 90 min) and processed as described in *Materials and Methods* and with the treatments (a, b, or c) as indicated (lanes 3–6 and 9): a, undigested control; b, digestion with *Bam*HI; c, digestion with *Eco*RI and *Bam*HI. Lanes 1 and 7, untreated DNA; lane 10, *Hin*dIII fragments of phage λ DNA (sizes in kilobases at right). Fragments diagnostic for repair are 4.0 and 3.2 kb. The autoradiogram was intentionally overexposed to show that the heteroduplex preparation contained some *Eco*RI-sensitive DNA (lane 2c), presumably produced by occasional extensive DNA polymerase I synthesis occurring during prelabeling. Repair was quantified by densitometry of this exposure for the 3.2-kb fragment and of a briefer exposure for the 7.2-kb DNA in lanes c. Values (shown below lanes c) have been corrected for nonincubated DNA (1%, lane 2c). The radiolabeled 7.2-kb DNA was accompanied by the excess unlabeled mp2 DNA in lanes b and so migrated more rapidly than in lanes c. RF II, replicative form II (nicked circular double-stranded).

poration values of about 20. Therefore, the DNA synthesis in these repair-diagnostic fragments was mismatch-stimulated. *Xenopus* egg extracts can convert ssDNA to form I DNA even without added primers (17). However, no localized synthesis was observed with ssDNA (Fig. 3*c*), a potential minor contaminant of heteroduplex preparations, or with homoduplex DNA (Fig. 3*b*). We conclude that the presence

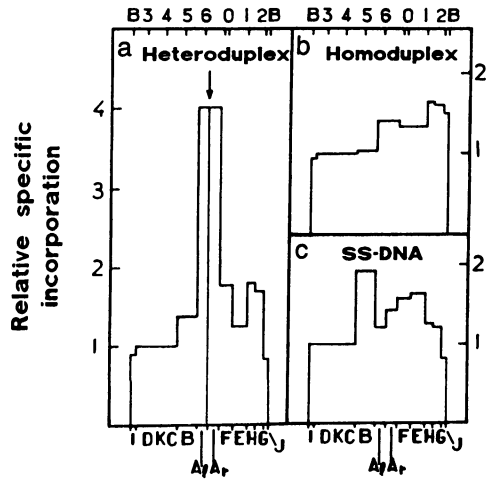

FIG. 3. A mismatched base pair provokes localized DNA synthesis. Reactions were for 20 min and included [α-^{32}P]dCTP at 3400 cpm/pmol of total dCTP and 8.5 μM mp2/mp1 heteroduplex DNA (*a*), 8.5 μM mp1/mp1 homoduplex DNA (*b*), or 6 μM mp2 ssDNA (*c*). Postreaction digestion was with *Eco*RI as the repair-diagnostic enzyme and with *Bam*HI and *Taq* I. The value for fragment A was calculated from the sum of specific incorporation into fragments A, A_l, and A_r. Fragments C and D were not well resolved and their values were grouped together with that of the intervening fragment K (fragment DKC). Relative specific incorporation values in individual segments of the molecule were normalized to the specific incorporation in fragment DKC. Fragment designations on the bottom axis are as shown in Fig. 1*b*. Map positions (kb) are indicated on the top axis; B, the *Bam*HI site (position 2221). Arrow and corresponding vertical line indicate mismatch position.

of a mismatch provokes DNA synthesis that occurs preferentially in the region containing the mismatch.

Fig. 4 shows the results obtained with a heteroduplex with a 2-base addition (+GC) in one strand (substrate 3, Fig. 1*a*, with the addition at a position comparable to the *Eco*RI site in mp2, Fig. 1*b*). Repair synthesis was increased and was localized in a region spanning at least 645 bp (fragments H through J) containing the unpaired bases. This profile is similar to that observed with the single base-pair mismatch (Fig. 3*a*) and therefore, as for the *E. coli mutHLS* system, one repair system in *Xenopus* may address both single-base and frameshift mismatches.

Mismatch-Localized Synthesis Is Enhanced in Repaired Molecules. The above results show that the extract has both an activity that converts heteroduplex DNA to homoduplex DNA and an activity that generates mismatch-localized DNA synthesis. To determine whether the repair was caused by the localized synthesis, the pattern of DNA synthesis was examined in repaired molecules that were isolated from the total population of extract-treated heteroduplex molecules. Unlabeled heteroduplex DNA (mp2B/mp2, with a T·G mismatch in the *Bgl* II/*Acc* I site, substrate 4, Fig. 1*a*) and [^{32}P]dNTP were incubated with the extract. The DNA was extracted and probed with *Acc* I and/or *Bgl* II, and then repaired molecules in the form of the repair-diagnostic fragments were gel-purified from the unrepaired 7.2-kb linear molecules. The isolated repaired or unrepaired molecules were then digested with a set of restriction enzymes for the analysis of the intramolecular distribution of synthesis. The profile and amplification of DNA synthesis for the total population of molecules (Fig. 5*a*), repaired and unrepaired, were similar to those observed for the heteroduplexes mp2/mp1 (Fig. 3*a*) and mp18N/mp18 (Fig. 4). Maximum synthesis occurred in the mismatch-bearing fragment H and adjacent fragments (Fig. 5*a*). For the isolated repaired molecules (4.7 kb and 2.5 kb), the relative specific incorporation in regions flanking the mismatch was increased at least 40- to 100-fold versus distal regions of the molecule (Fig. 5 *c* and *d*), thus showing that repaired molecules display mismatch-localized synthesis.

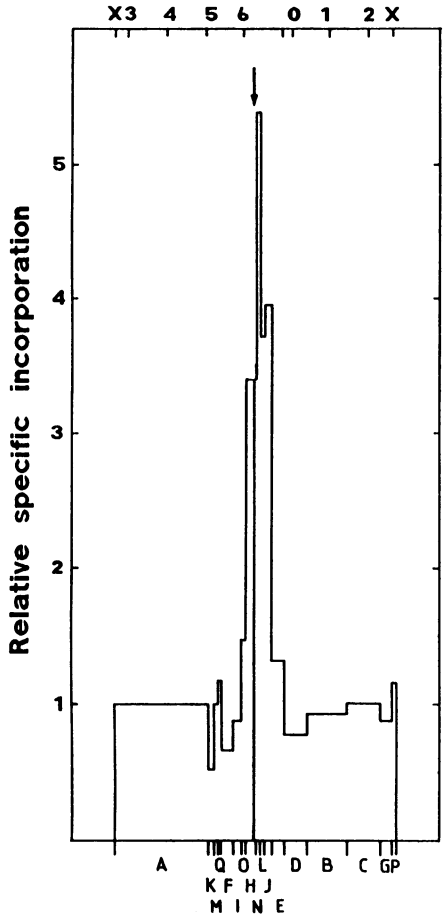

FIG. 4. Unpaired bases provoke localized DNA synthesis. Reaction with 36 μM mp18N/mp18 heteroduplex DNA was for 20 min and included [α-^{32}P]dCTP at 12,400 cpm/pmol. DNA was digested with the repair-diagnostic enzymes *Sal* I and *Nru* I and with *Xmn* I and *Hae* III; relative specific incorporation is with respect to *Xmn* I–*Hae* III fragment A. The (+GC) addition mismatch is at position 6266 in *Hae* III fragment H (arrow); X, the *Xmn* I site at position 2651.

Extent of Mismatch-Specific Repair. Analysis of the above data permits an estimation of the proportion of repair that occurred by mismatch-dependent DNA synthesis. In the experiments that included [^{32}P]dNTP (such as Figs. 3–5), it cannot necessarily be assumed that the [^{32}P]dNTP equilibrates with the endogenous 50 μM dNTP. The population of repaired molecules might include a large fraction of nonspecifically repaired DNA (X_n) and a small fraction of specifically repaired DNA (X_s) in which the specific incorporation is high ($X_s + X_n = 1$). It can be shown that a minimum value for X_s is typically 0.1–0.3.† However, the pattern of intramolecular distribution of DNA synthesis in repaired fragments (such as in Fig. 5 *c* and *d*) fixes an upper limit to their overall specific incorporation. This means that there must be a larger proportion of specifically repaired molecules; for example, for the experiment of Fig. 5, $X_s \geq 0.8$ (P.B., unpublished analysis). Finally, if it is assumed that there is one dNTP pool, the background level of base replacement can be determined directly; for Fig. 5, this value is 0.02%. Assuming that this represents random synthesis, then, among the total population of molecules, the fraction in which a given base is replaced, such as at the mismatch position, is necessarily also 0.02%. Therefore, with these assumptions, for the experiment of Fig. 5, >99% of the repaired molecules were repaired by a mismatch-specific system.

†If we define f as the fraction of DNA in the repaired fragments and S as the ratio of the specific incorporation in the repaired fragments to that found either in homoduplex DNA or in regions of the heteroduplex not showing mismatch-stimulated synthesis, then when $S >> X_n$, $X_s/X_n \geq f \cdot S$ (P.B., unpublished derivation). For example, for Fig. 5, $f = 0.06$, $S = 7$, and so $X_s \geq 0.3$.

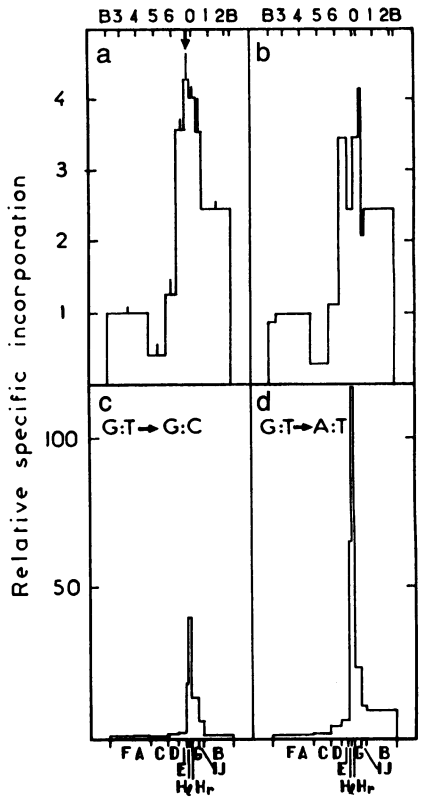

FIG. 5. DNA synthesis in repaired and unrepaired heteroduplex DNA. Reaction with 20 μM mp2B/mp2 heteroduplex DNA was for 20 min and included [α-^{32}P]dATP and [α-^{32}P]dCTP at 15,000 cpm/pmol. After extraction, the DNA was divided into three reactions: 1, *Bam*HI and *Acc* I for T·G → T·A repair; 2, *Bam*HI and *Bgl* II for T·G → C·G repair; 3, *Bam*HI, *Acc* I, and *Bgl* II to examine unrepaired DNA. Digestions also included plasmid pHV33 (22) and/or mp18 DNA to verify complete digestion by the enzymes. The 7.2-kb linear DNA and the 4.7- and 2.5-kb repair-diagnostic fragments from each of the three reactions were individually gel-purified (GeneClean; Bio 101, La Jolla, CA) and then digested with *Ban* II, *Eco*RI, and *Dra* I. (Digestions of the unrepaired 7.2-kb DNA also included *Xmn* I to produce fragments I and J, since uncleaved fragment IJ comigrates with fragment H. *Xmn* I digestion also cleaves fragment FA into F and A.) (*a*) Specific incorporation values for each fragment were added together and relative specific incorporation (and percent error) was calculated from the average values for the three reactions. Fragment IJ includes values for fragments IJ, I, and J; FA includes FA, F, and A; H includes H, H_l, and H_r. (*b*) Relative specific incorporation in unrepaired 7.2-kb linear DNA from reaction 3. (*c* and *d*) Relative specific incorporation in the diagnostic 4.7- and 2.5-kb fragments produced by *Acc* I (reaction 1, *c*) or by *Bgl* II (reaction 2, *d*). Values in *c* for fragments FA, C, D, E, and B and in *d* for fragments FA, C, D, E, and IJ represent maximum values, as radioactivity in these fragments was not different from background. Relative incorporation is with respect to fragment FA for *a*, *c*, and *d* and with respect to fragment A for *b*. See Fig. 3 legend for notation.

A Mismatch Can Provoke Localized Synthesis But Remain Unrepaired. The distribution of nucleotide incorporation in unrepaired heteroduplex DNA was also determined. The profile of relative incorporation (Fig. 5*b*) is similar to that for the sum of the fractionated reaction products (Fig. 5*a*). The increased synthesis observed in fragments H_l and H_r shows that even within 150-bp of the mismatch, specific incorporation occurred that did not result in mismatch repair. With the +2 addition heteroduplex, similar distributions of synthesis were also observed for repaired and unrepaired DNA

(data not shown). We infer that for some molecules, mismatch-provoked repair synthesis was initiated at some distance from the mismatch but not completed. Hence, intermediates in the repair process may have been identified by this experimental approach.

DISCUSSION

The results reported here demonstrate a vertebrate DNA-repair activity that responds to mismatches or unpaired bases. Whether or not accompanied by repair, mismatch-provoked nucleotide incorporation was generally observed at distances including at least 0.5 kb on either side of the mismatch. For isolated repaired molecules, the most pronounced region of increased synthesis included not more than about 150 bp on either side. It remains to be determined whether an individual mismatch-repair event involves contiguous synthesis on both sides of the mismatch or synthesis involving only one side, either the left or the right. The incidence of initiation of DNA synthesis and the likelihood that the synthesis will result in successful repair apparently decrease with the distance from the mismatch (Fig. 5). Thus only initiations of synthesis within a limited distance (<150 bp) from the mismatch are likely to produce a repaired molecule. Whatever the mechanism of initiation, the initial steps in repair are not rate-limiting, since substantial mismatch-induced synthesis did not result in repair of the mismatch but was found in apparent intermediates in the repair process (Fig. 5*b*).

Several alternatives could account for these intermediates. (*i*) As has been proposed for *E. coli* mismatch repair (3), initiation might occur via interaction between a mismatch-binding protein and an endonuclease acting at some distance from the mismatch. If excision repair proceeds from the nick toward the mismatch, competing ligation may then have stopped repair synthesis that needed more than about 150 bp of synthesis to reach the mismatch. (*ii*) Without a strand-discrimination signal, unrepaired molecules with mismatch-stimulated synthesis would also include those for which DNA synthesis was initiated close to the mismatch but on the 3′ side and thus proceeding in the direction away from the mismatch. (*iii*) A helicase-mediated, mismatch-stimulated melting might enable initiation of DNA synthesis on either or both strands or might enable an endonucleolytic cleavage on either strand followed by strand-replacement synthesis. Mismatch-stimulated melting has been postulated for *E. coli* mismatch repair (23) and may be adequate for the removal of newly synthesized Okazaki fragments bearing a mismatch caused by a replication error. (*iv*) A double-strand break or gap (caused by endonucleolytic attack on both mismatched strands) that is immediately repaired by recombination (24, 25) could also result in localized synthesis with or without mismatch repair. (*v*) A short-patch repair system might generate the successfully repaired molecules, while an uncompleted long-patch repair may be responsible for the intermediates.

Estimates of the size of mismatch-repair tracts in diverse experimental systems extend from as little as a few bases for VSPMR in *E. coli* (26, 27) up to several kilobases for *E. coli* LPMR (19, 23, 28, 29) and for yeast (30–32). The experiments reported here show that the synthesis associated with successful mismatch repair may range from very short to 0.3 kb (Fig. 5 *c* and *d*). However, the size of the region involved in mismatch-stimulated synthesis for the complete population of molecules may extend from a few hundred base pairs to more than a kilobase of DNA (Fig. 5*a*). Neither these nor any other published experiments enable a determination of the actual contiguous repair patch size for individual molecules.

The *in vitro* eukaryotic system described here for specific mismatch repair permits the assay of signals such as methylation or nicks for their ability to direct strand-specific mismatch correction (33) and enables testing for recombinational repair of mismatches.

This work was supported by Association pour la Recherche sur le Cancer Contract 6159, European Economic Community Contract BI6-0154-F, and Caisse Nationale de l'Assurance des Travailleurs Salariés Grant 86-3-34-1-E; P.B. was also supported by the Foundation Philippe.

1. Claverys, J. P. & Lacks, S. A. (1986) *Microbiol. Rev.* **50,** 133–165.
2. Radman, M. & Wagner, R. (1986) *Annu. Rev. Genet.* **20,** 523–538.
3. Modrich, P. (1987) *Annu. Rev. Biochem.* **56,** 435–466.
4. Meselson, M. (1988) in *The Recombination of Genetic Material*, ed. Low, K. B. (Academic, New York), pp. 91–113.
5. Jones, M., Wagner, R. & Radman, M. (1987) *Cell* **50,** 621–626.
6. Radman, M. (1988) in *Genetic Recombination*, eds. Kucherlapati, R. & Smith, G. R. (Am. Soc. of Microbiol., New York), pp. 169–192.
7. Holliday, R. (1964) *Genet. Res.* **5,** 282–304.
8. White, J. H., Lusnak, K. & Fogel, S. (1985) *Nature (London)* **315,** 350–352.
9. Leblon, G. & Rossignol, J.-L. (1973) *Mol. Gen. Genet.* **122,** 165–182.
10. Muster-Nassal, C. & Kolodner, R. (1986) *Proc. Natl. Acad. Sci. USA* **83,** 7618–7622.
11. Abastado, J.-P., Cami, B., Dinh, T. H., Igolen, J. & Kourilsky (1984) *Proc. Natl. Acad. Sci. USA* **81,** 5792–5796.
12. Hare, J. T. & Taylor, J. H. (1985) *Proc. Natl. Acad. Sci. USA* **82,** 7350–7354.
13. Brown, T. C. & Jiricny, J. (1988) *Cell* **54,** 705–711.
14. Gurdon, J. B. & Wickens, M. P. (1983) *Methods Enzymol.* **101,** 370–386.
15. Zierler, M. K., Marini, N. J., Stowers, D. J. & Benbow, R. M. (1985) *J. Biol. Chem.* **260,** 974–981.
16. Almouzni, G. & Méchali, M. (1988) *EMBO J.* **7,** 665–672.
17. Méchali, M. & Harland, R. M. (1982) *Cell* **30,** 93–101.
18. Messing, J. (1983) *Methods Enzymol.* **101,** 20–78.
19. Lu, A-L., Clark, S. & Modrich, P. (1983) *Proc. Natl. Acad. Sci. USA* **80,** 4639–4643.
20. Davis, R. W., Botstein, D. & Roth, J. R. (1980) *Advanced Bacterial Genetics* (Cold Spring Harbor Lab., Cold Spring Harbor, NY).
21. Vovis, G. F., Horiuchi, K., Hartman, N. & Zinder, N. D. (1973) *Nature (London) New Biol.* **246,** 13–16.
22. te Riele, H., Michel, B. & Ehrlich, S. D. (1986) *EMBO J.* **5,** 631–637.
23. Längle-Rouault, F., Maenhaut-Michel, G. & Radman, M. (1987) *EMBO J.* **6,** 1121–1127.
24. Wagner, R., Dohet, C., Jones, M., Doutriaux, M.-P., Hutchinson, F. & Radman, M. (1984) *Cold Spring Harbor Symp. Quant. Biol.* **49,** 611–615.
25. Hastings, P. J. (1984) *Cold Spring Harbor Symp. Quant. Biol.* **49,** 49–53.
26. Lieb, M. (1983) *Mol. Gen. Genet.* **191,** 118–125.
27. Jones, M., Wagner, R. & Radman, M. (1987) *J. Mol. Biol.* **194,** 155–159.
28. Wagner, R. & Meselson, M. (1976) *Proc. Natl. Acad. Sci. USA* **73,** 4135–4139.
29. Lu, A.-L., Welsh, K., Clark, S., Su, S.-S. & Modrich, P. (1984) *Cold Spring Harbor Symp. Quant. Biol.* **44,** 589–596.
30. Bishop, D. K. & Kolodner, R. D. (1986) *Mol. Cell. Biol.* **6,** 3401–3409.
31. Borts, R. H. & Haber, J. E. (1987) *Science* **237,** 1459–1465.
32. Symington, L. S. & Petes, T. D. (1988) *Mol. Cell. Biol.* **8,** 595–604.
33. Brooks, P., Dohet, C., Petranovic, M. & Radman, M. (1988) in *Mechanisms and Consequences of DNA Damage Processing*, UCLA Symposium on Molecular and Cellular Biology, New Series, eds. Friedberg, E. & Hanawalt, P. (Liss, New York), Vol. 83, pp. 167–171.